

NEUROGENESIS IN THE RAT PRIMARY OLFACTORY CORTEX

SHIRLEY A. BAYER

Department of Biology, Indiana-Purdue University, 1125 East 38th Street, Indianapolis, IN 46223, U.S.A.

(Accepted 16 December 1985)

Abstract—Neurogenesis in the rat primary olfactory cortex was examined with [³H]thymidine autoradiography. The experimental animals were the offspring of pregnant females given an injection of [³H]thymidine on two consecutive gestation days. Nine groups of embryos were exposed to [³H]thymidine on E13–E14, E14–E15, . . . E21–E22, respectively. On P60, the percentage of labeled cells and the proportion of cells originating during 24 hr periods were quantified at selected anatomical levels of the anterior and posterior piriform cortex, dorsal lateral peduncular cortex, and posterior two-thirds of the ventral agranular insular cortex. Throughout most of the primary olfactory cortex, deep cells are generated earlier than superficial cells: the 'inside-out' pattern. Neurons in the anterior (prepiriform) cortex are located lateral to the caudal anterior olfactory nucleus and olfactory tubercle, and are generated mainly between E14 and E18 in a caudal (older) to rostral (younger) neurogenetic gradient. Neurons in the posterior (periamygdaloid) cortex are located lateral to the caudal olfactory tubercle and amygdala, and are generated mainly between E14 and E17 simultaneously along the rostrocaudal plane. Superficial cells in the piriform cortex have some additional neurogenetic gradients; ventromedial cells forming transition zones with either the olfactory tubercle or amygdala originate earlier than cells located dorsally and laterally. In the posterior piriform cortex, younger neurons are located at middle dorsoventral levels while older neurons lie above and below. Neurons in the dorsolateral peduncular cortex originate between E14 and E20 in a caudal to rostral gradient of neurogenesis; caudal parts also have a lateral to medial neurogenetic gradient. The most lateral part of the dorsolateral peduncular cortex is unique and does not have the typical 'inside-out' cortical neurogenetic gradient. Neurons in the ventral agranular insular cortex (area 13) originate mainly between E15 and E17 in combined caudal to rostral and ventral to dorsal neurogenetic gradients. The neurogenetic gradients in the primary olfactory cortex, along with patterns of neurogenesis throughout the olfactory projection field are related to the termination patterns of afferents from the main olfactory bulb.

Key words: Piriform cortex, Insular cortex, Primary olfactory cortex, [³H]Thymidine autoradiography, Neurogenesis.

The primary olfactory cortex is defined as that part of the telencephalic cortical mantle which gets a direct projection from the main olfactory bulb. The projection to the piriform cortex was first described by LeGros Clark and Meyer³⁷ and was confirmed by several experimental anatomical studies in the 1960s and early 1970s.^{16,22,29,45,46,64} Many studies on various aspects of the projection are in the recent neuroanatomical literature.^{11,12,17,19,25,26,40–42,48,49,55–58,60,61}

The entorhinal cortex, especially the ventral lateral part, also receives direct olfactory input.^{11,12,17,29,33,41,46,48,57,58,60,61,64} Finally, a few of the most recent reports indicate that the posterior two-thirds of the ventral agranular insular cortex in the rhinal sulcus receives direct olfactory input.^{12,18,41,57–59} In macrosmatic mammals, the primary olfactory cortex makes up a substantial part of the cerebral cortex. In the rat it forms the entire ventrolateral wall of the telencephalon.

In contrast to the wealth of anatomical literature, only two studies have been published on neurogenetic patterns in the primary olfactory cortex. Pulse labeling with single injections of [³H]thymidine was used to establish approximate times for neuronal birth dates in the piriform cortex of the mouse; the results were reported in an abstract.³² Bayer⁴ quantified the timetables of neurogenesis in the entorhinal cortex using comprehensive labeling with multiple injections of [³H]thymidine. This method was introduced by Bayer and Altman¹⁰ and allows an accurate delineation of both the onset and cessation of neurogenesis as well as the determination of the proportion of neurons that originate during single days of embryonic life. The comprehensive labeling method has been used to quantify neurogenesis throughout the olfactory system, including the olfactory bulb,⁶ olfactory tubercle,⁸ anterior olfactory nucleus,⁹ cortical nuclei in the amygdala,⁵ and entorhinal cortex;⁴ this paper completes the series. The major finding in all these studies is that neurogenetic timetables correlate with patterns of anatomical connections.

EXPERIMENTAL PROCEDURES

The experimental animals were the offspring of Purdue-Wistar timed-pregnant rats given 2 s.c. injections of [³H]thymidine (Schwarz-Mann; sp. act. 6.0 Ci/mM; 5 µCi/g body wt) to insure com-

prehensive cell labeling. The injections (given between 9 and 11 a.m.) to an individual animal were separated by 24 hr. Two or more pregnant females made up each injection group. The onset of the [^3H]thymidine injections was progressively delayed by 1 day between groups (E13–E14, E14–E15, . . . E21–E22). The day the females were sperm positive was designated embryonic day one (E1). Normally, births occur on E23, which is also designated as postnatal day zero (P0). All animals were perfused through the heart with 10% neutral formalin on P60. The brains were kept for 24 hr in Bouin's fixative, then were transferred to 10% neutral formalin until they were embedded in paraffin. The brains of at least six animals from each injection group were blocked coronally according to the stereotaxic angle of the Pellegrino *et al.*⁴⁴ atlas. Every 15th section (6 μm) through the olfactory peduncle was saved. Slides were dipped in Kodak NTB-3 emulsion, exposed for 12 weeks, developed in Kodak D-19, and post-stained with hematoxylin and eosin.

The primary olfactory cortex extends nearly 11 mm (from A11.8 to A1.2) along the ventro-lateral telencephalic wall. Sections were selected for quantitative analysis at 11 anteroposterior levels (approximately one sample for each mm). Cells were counted microscopically at $\times 312.5$ in unit areas set off by an ocular grid (0.085 mm²) or in strips (0.29 mm wide). For quantification, all neurons within a designated area were assigned to one of two groups, labeled or nonlabeled. Cells with reduced silver grains overlying the nucleus in densities above background levels were considered labeled; obvious endothelial and glial cells were excluded. The proportion of labeled cells (% labeled cells/total cells) was then calculated from these data.

The determination of the proportion of cells arising (ceasing to divide) on a particular day utilized a modification of the progressively delayed comprehensive labeling procedure,¹⁰ and is described in detail elsewhere.^{5,6} Briefly, a progressive drop in the proportion of labeled neurons from a maximal level (>95%) in a specific population indicates that the precursor cells are producing nonmitotic neurons. By analyzing the rate of decline in labeled neurons, one can determine the proportion of neurons originating over blocks of days (or single days) during development. Table 1 shows the data and calculations for the superficial cells of the piriform cortex at level A11.2.

Throughout the quantitative analysis, it was noted that trends in cell labeling within animals were very consistent. For example, in the superficial cells in layer II of the posterior piriform

Table 1. Neurogenesis of the superficial cells in the anterior piriform cortex (A11.2)

Injection group	N	% Labeled cells*	Day of origin	% Cells originating†
E14–E15	7	(A) 99.43 \pm 0.53	E14	1.76 (A–B)
E15–E16	6	(B) 97.67 \pm 1.51	E15	21.84 (B–C)
E16–E17	12	(C) 75.83 \pm 4.63	E16	31.50 (C–D)
E17–E18	9	(D) 44.33 \pm 7.62	E17	21.83 (D–E)
E18–E19	6	(E) 22.50 \pm 6.35	E18	11.67 (E–F)
E19–E20	6	(F) 10.83 \pm 2.23	E19	8.33 (F–G)
E20–E21	7	(G) 2.50 \pm 2.23	E20	2.50

* $\bar{X} \pm \text{S.D.}$

† Graphed in Fig. 2 (top).

The data for the superficial cells in the anterior piriform cortex at A11.2 are given as an example of how the data are derived for presentation in the bar graphs used throughout the figures in this paper. *N* refers to the number of animals analyzed in each injection group. The same number of animals is used to collect data for all graphs throughout this paper. The % labeled cells is the group mean and standard deviation for the raw data (counts of the % of labeled cells to total cells) for each injection group. The standard deviations are typical of the variability seen throughout the data collection. The % cells originating column lists the data that are presented in the bar graph (Fig. 2, top). To get the height of the second bar, for example, the proportion of labeled cells in injection group E15–E16 (entry B, column 3) is subtracted from the % labeled cells in injection group E14–E15 (entry A, column 3) to get the proportion of cells originating during the day on E14 (1.76%).

cortex (Fig. 3), the percentage of labeled cells in the intermediate area tended to be slightly higher than the percentage of labeled cells either above or below this area. However, variability between animals in an injection group were large enough to mask this trend. Cell labeling patterns were analyzed with the sign test,¹⁵ a non-parametric test suited to the type of data collected throughout the study. The sign test determines the consistency of sequential neuron production between paired locations within individual animals. The comparisons are grouped into three categories: (1) $X > Y$, '-' comparison; (2) $X < Y$, '+' comparison; (3) $X = Y$ '0' comparison. The zero comparisons are discarded and, depending on the total number of remaining '+' and '-' comparisons, either a binomial distribution or a normal approximation is used to calculate probabilities (P). The graphs throughout this report show the more variable group data rather than consistent trends in data from individual animals. Consequently, some of the statistically significant neurogenetic gradients (between dorsal, intermediate and ventral areas of layer II, Fig. 3) are not conspicuous in the group data.

RESULTS

Time of origin of neurons in the piriform cortex

Cytoarchitectonic considerations. The largest part of the primary olfactory cortex is taken up by the piriform cortex, Krieg's^{34,35} areas 51a and 51b. The piriform cortex extends nearly 7.4 mm from the ventral-lateral transition area surrounded by the anterior olfactory nucleus (approximately A11.8⁴⁴) to A4.4. It forms the ventral lateral wall of the telencephalon, just beneath the rhinal sulcus (drawings, Figs 1-3). Due to its specific neurogenetic characteristics, the piriform cortex does not extend into the rhinal sulcus. Most anatomists consider that the piriform cortex has three cell layers and an external plexiform layer I. Layer II contains not only small pyramidal cells,^{24,43,62,63} but also semilunar cells whose dendrites form a semicircle in layer I, and polygonal cells of variable shape. All of these neurons send dendrites to layer Ia which contains the mitral cell axon terminals. Layer III contains medium-sized pyramidal cells which often have branched

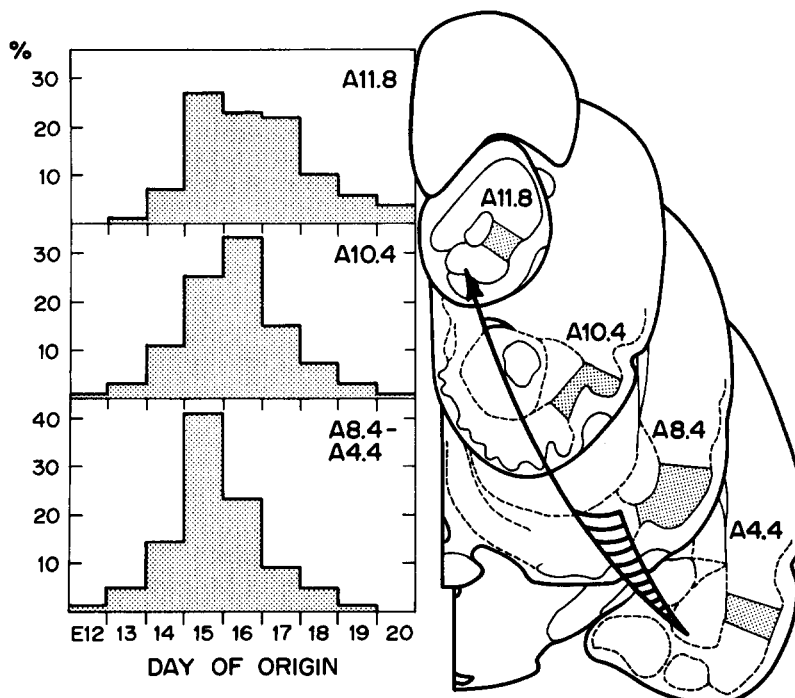


Fig. 1. The time of origin of neurons throughout the rostrocaudal extent of the piriform cortex. Neurons were counted in strips through the shaded areas shown in the drawings; all cell counts were combined. The bar graphs represent the proportion of neurons originating during single embryonic days. Neurons between levels A8.4 and A4.4 originate simultaneously (data are combined in the lower graph) and earlier than neurons at more anterior levels.

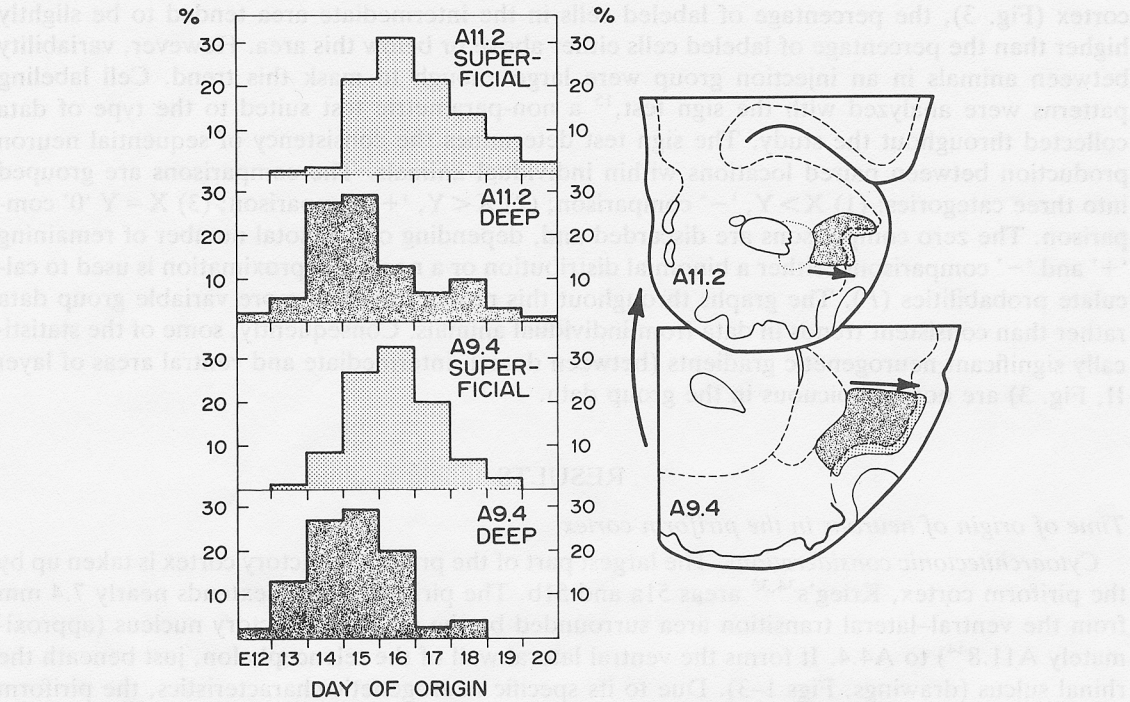


Fig. 2. Neurogenesis in the anterior piriform cortex. Counts of neurons in layers II (superficial) and III (deep) were done separately. The bar graphs represent the proportion of cells originating during single embryonic days. Table 1 indicates how the data were calculated for the top graph. Deep cells originate earlier than superficial cells (arrows in drawings), while cells at level A9.4 tend to be slightly older than those at level A11.2 (arrow between drawings).

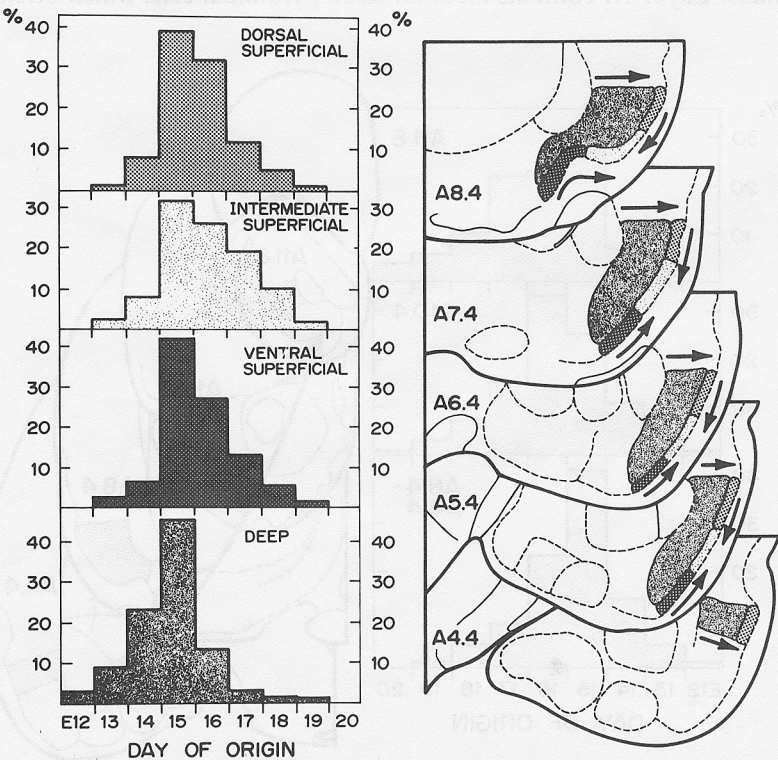


Fig. 3. Neurogenesis in the posterior piriform cortex. Neurons originate simultaneously between levels A8.4 and A4.4, and all graphs show combined data. Bar graphs represent the proportion of cells originating during single embryonic days. Deep cells throughout (bottom graph) originate earlier than superficial cells (arrow pointing toward surface in drawings). There is a tendency for intermediately located superficial cells (graph second from top) to be slightly younger than cells above and below (arrows point toward these cells in drawings).

apical dendrites. Double-tufted cells, containing profusely branched apical and basal dendrites are also found here. Most cells in layer III also have dendrites extending to the olfactory terminal zone. Large pyramidal cells and horizontal cells are found in layer IV. In the rat, the cell density in layer IV is quite sparse in 6 μm sections, therefore the quantification of layers III and IV are combined as the 'deep cells'.

O'Leary⁴³ describes anterior and posterior differences in the cytoarchitectonics of the piriform cortex: layer II is thicker anteriorly and contains smaller cells than those found posteriorly (compare the cell sizes in the photomicrographs in Figs 4 and 6). The posterior piriform cortex begins at the level of the interface between the posterior olfactory tubercle and the anterior amygdala (top drawing, Fig. 3) and is characterized by a thinner layer II (Fig. 4) and a more densely packed layer III–IV.

Neurogenesis along the rostrocaudal axis. Cell counts of neurons in layers II and III–IV were combined at 10 levels between A11.8 and A4.4 to present an overview in Fig. 1 of the major neurogenetic gradients along the rostrocaudal axis. These gradients served to differentiate the anterior and posterior parts of the piriform cortex. The sign test shows that all neurons between levels A8.4 and A4.4 originate simultaneously, and these data are combined in the bottom graph (Fig. 1). Approximately 62% of the population arises between E12 and E15, significantly earlier ($P < 0.01$) than more rostral cells. The posterior piriform cortex was considered to be the entire caudal expanse of cortex that lies lateral to the amygdala and caudal parts of the olfactory tubercle. This is also called periamygdaloid cortex by Valverde^{62,63} and piriform cortex medialis by Gray.²⁴ Beginning at level A9.4, a stepwise caudal to rostral gradient is found in which neurons at A9.4 originate significantly earlier ($P < 0.035$) than those at A10.4, and those at A10.4 (middle graph, Fig. 1) significantly earlier ($P < 0.0001$) than those at A11.2. Both deep cells ($P < 0.02$) and superficial cells ($P < 0.0001$) have significant caudal to rostral neurogenetic gradients (Fig. 2). Beyond A11.2, the piriform cortex merges with the ventral–lateral transition area associated with the anterior olfactory nucleus. Neurogenesis in the ventral–lateral transition area continues the caudal (older) to rostral (younger) gradient (top graph, Fig. 1): 66% of the population originates late, between E16 and E20. The part of the piriform cortex showing the more pronounced caudal to rostral gradient (A9.4 and forward) is designated anterior piriform cortex according to the terminology of Gray;²⁴ Valverde^{62,63} calls this the prepiriform cortex.

Superficial–deep gradients. Between levels A11.2 and A9.4, the anterior piriform cortex widens in the dorsoventral dimension. For quantification, cells in layers II and III–IV were counted separately in dorsal and ventral strips. The sign test shows no differences between the time of origin in dorsal vs ventral strips so the data are combined in Fig. 2. At levels A11.2 and A9.4, deep cells originate significantly earlier than superficial cells ($P < 0.0001$) in a prominent deep (older) to superficial (younger) neurogenetic gradient (Fig. 2). For example, at level A11.2, 65% of the cells in layers III–IV originate between E12 and E15, while 76% of the layer II cells are generated between E16 and E20.

Throughout the posterior piriform cortex (drawings, Fig. 3), cells in layers III–IV were counted separately from cells in layer II in three strips, dorsal, intermediate and ventral. The sign test shows that the deep cells in all three strips are not significantly different so the data in the bottom graph of Fig. 3 are combined. As in the anterior piriform cortex, deep cells originate significantly ($P < 0.0001$) earlier than superficial cells in a very strong deep to superficial gradient. Approximately 82% of the deep cells are generated between E12 and E15, while most of the superficial cells in dorsal, intermediate and ventral locations are generated on or after E15.

Intrinsic layer II neurogenetic gradients. Layer II cells in the posterior piriform cortex show an additional neurogenetic gradient along the dorsoventral axis. The areas shown in Fig. 4 are from dorsal (Fig. 4A), intermediate (Fig. 4B) and ventral (Fig. 4C) parts of layer II; the highest density of labeled cells is found in the intermediate area. Neurogenesis in all parts of layer II occurs mainly on E16 and E17 (three top graphs, Fig. 3). On and after E17, significantly less ($P < 0.019$) neurogenesis occurs in dorsal and ventral areas (21 and 18%, respectively) than in the intermediate area (32%). This is an example of a young center 'sandwich' type neurogenetic gradient.

In both the anterior and posterior parts of the piriform cortex, layer II forms transition zones as it extends farther ventrally and medially than layers III and IV (drawings, Fig. 5). Ventral extensions are prominent between A11.2 and A9.4 as zones of tightly packed small cells (Fig. 6B)

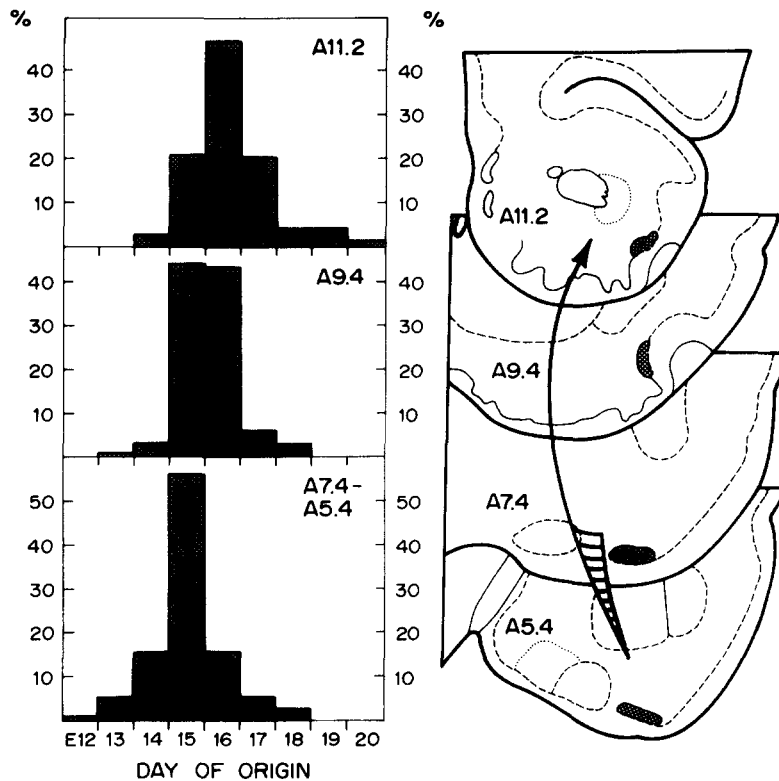


Fig. 5. Neurogenesis in the ventromedial superficial cells forming transition areas to either the olfactory tubercle (two top graphs) or the amygdala (bottom graph). Cells were counted in the shaded areas indicated in the drawings. Bar graphs represent the proportion of neurons originating during single embryonic days. Neurons between levels A7.4 and A5.4 originate simultaneously (data are combined in the bottom graph) and earlier than those at more anterior levels (arrow between sections in drawings).

adjacent to the layer II cells in the olfactory tubercle. The ventromedial extension is reduced at A8.4, but it reappears at level A7.4 and extends throughout the posterior piriform cortex as a ventral lamina of tightly packed cells (Fig. 4D). These cells form a transition zone to the superficial cells of the anterior and posterolateral cortical amygdaloid nuclei. Gray²⁴ called these ventromedial specializations the subpiriform cortex.

All cells within the layer II transition zones were counted at six levels between A11.2 and A5.4. The sign test shows that neurons in the piriform-amygdaloid transition zone (A7.4-A5.4) originate simultaneously; consequently, the data in the bottom graph of Fig. 5 are combined. These cells originate significantly earlier ($P < 0.0001$) than those in the transition zone adjacent to the anterior piriform cortex. Here, neurons originate in a pronounced stepwise caudal to rostral neurogenetic gradient. Cells at A9.4 (middle graph, Fig. 5) originate significantly earlier than those at A10.4 ($P < 0.0001$); those at A10.4 significantly earlier than those at A11.2 ($P < 0.0001$; top graph, Fig. 5). These data repeat the pattern seen throughout the entire piriform cortex proper (Fig. 1). The caudal to rostral gradient is especially strong: in the posterior transition zone, 77% of the population originates between E13 and E15, while 76% of the population in the anterior transition zone at A11.2 originates between E16 and E19.

The cells in the posterior transition zone originate earlier than cells throughout layer II in the posterior piriform cortex (compare labeling levels in Fig. 4D with Fig. 4A-C). Similarly, Fig. 6 shows fewer labeled cells in the anterior transition zone (Fig. 6A) than in layer II in the anterior piriform cortex proper (Fig. 6B). The data for level A10.4 are shown in Fig. 7. (Other levels show similar data and are not illustrated.) While a few neurons are generated in all parts of layer II on E14, on and after E15 there is a distinct ventral to dorsal neurogenetic gradient. Neurons in the ventromedial transition zone (bottom graph) originate significantly earlier ($P < 0.003$) than those in the dorsal parts of layer II.

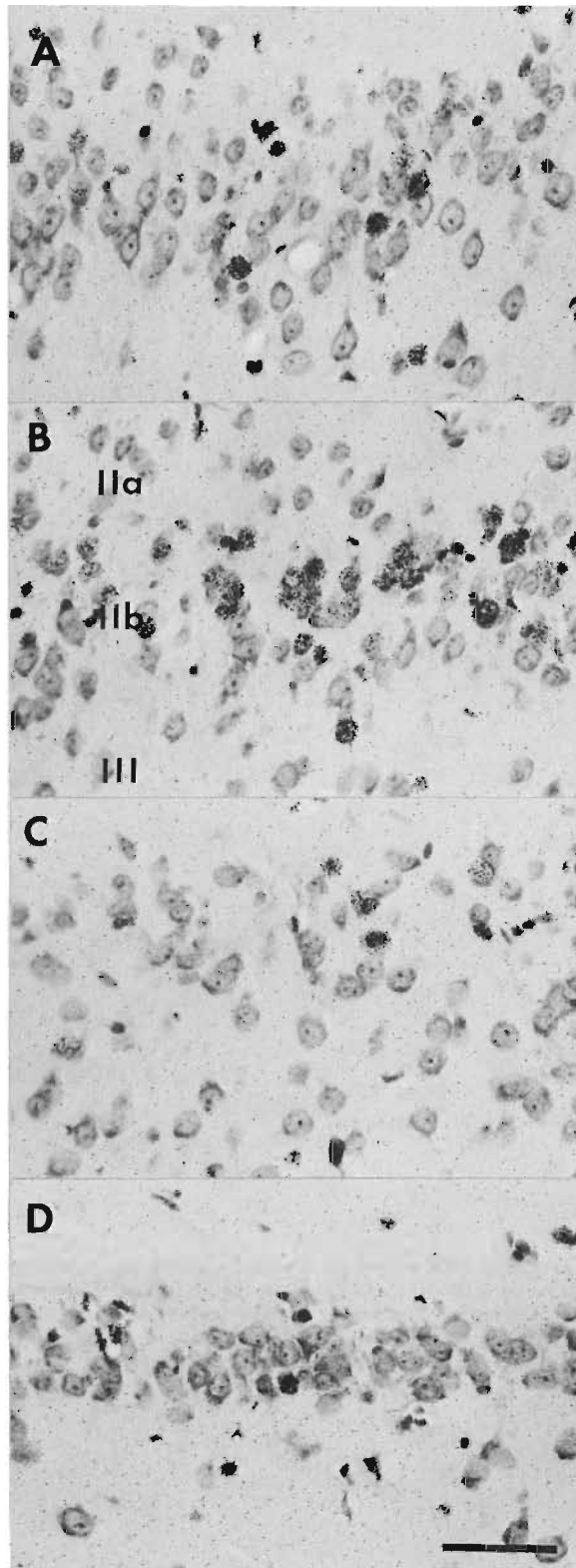


Fig. 4. Autoradiograms of layer II in the posterior piriform cortex at level A6.4 in an animal exposed to [^3H]thymidine on E17+E18 and killed on P60 (6 μm paraffin sections, hematoxylin and eosin, scale = 0.05 mm). The levels shown are: (A) dorsal; (B) intermediate; (C) ventral; (D) ventromedial transition area. Notice that only one labeled cell is seen in (D), while most labeled cells are seen in (B). The lamina in the intermediate area (B) is thicker, and can be subdivided into superficial (IIa) and deep (IIb) parts. Notice that IIa contains proportionately fewer labeled cells than IIb.

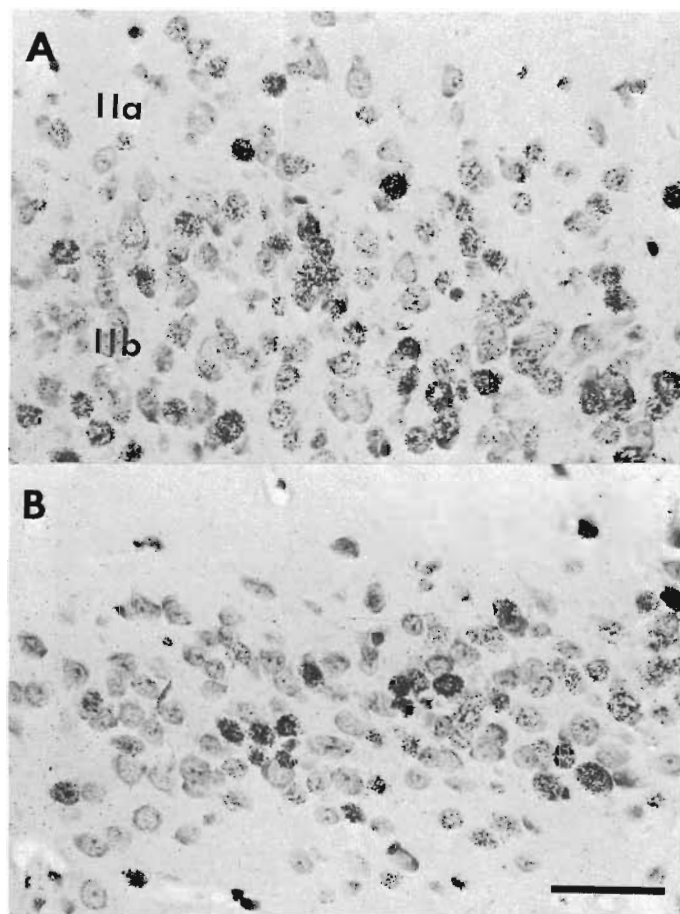


Fig. 6. Autoradiograms of superficial cells in the anterior piriform cortex at level A10.4 in an animal exposed to [^3H]thymidine on E16+E17 and killed on P60 (6 μm paraffin sections, hematoxylin and eosin, scale = 0.05 mm). Dorsal (A) areas have a higher proportion of labeled cells than ventral (B) areas. The dorsal area (A) is thicker and can be subdivided into superficial (IIa) and deep (IIb) parts; notice that layer IIa contains proportionately fewer labeled cells than IIb.

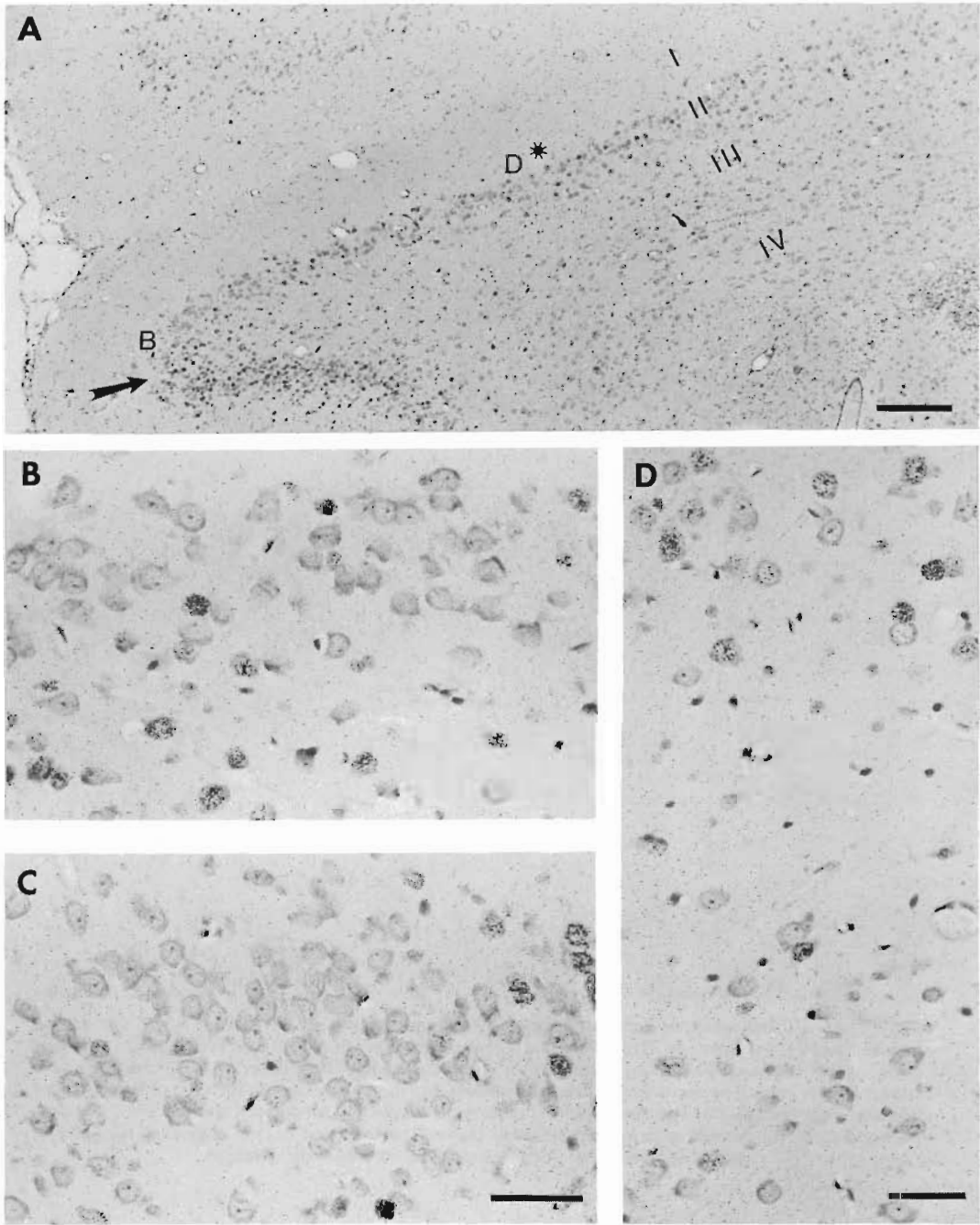


Fig. 8. Autoradiograms of the dorsolateral peduncular cortex in an animal exposed to [^3H]thymidine on E16+E17 and killed on P60 (6 μm paraffin sections, hematoxylin and eosin). The low magnification view in (A) (scale = 0.25 mm) shows the mediolateral extent of this area at level A11.2; Roman numerals (I–IV) indicate cortical layers. The arrow points to the junction with the ventrally positioned piriform cortex; at this point, the proportion of labeled superficial cells sharply decreases. The proportion of labeled superficial cells begins to increase medially (beneath asterisk). (B) High magnification view of the area just above the arrow in (A); superficial cells are mostly unlabeled, while deep cells still are labeled. (D) High magnification view of the area just below the asterisk in (A); deep cells are unlabeled, while superficial cells are mostly labeled. (C) High magnification view of a cluster of mostly unlabeled superficial cells at level A10.4, probably an extension of the early forming superficial cells at A11.2. Scales from (B) to (D) = 0.05 mm.

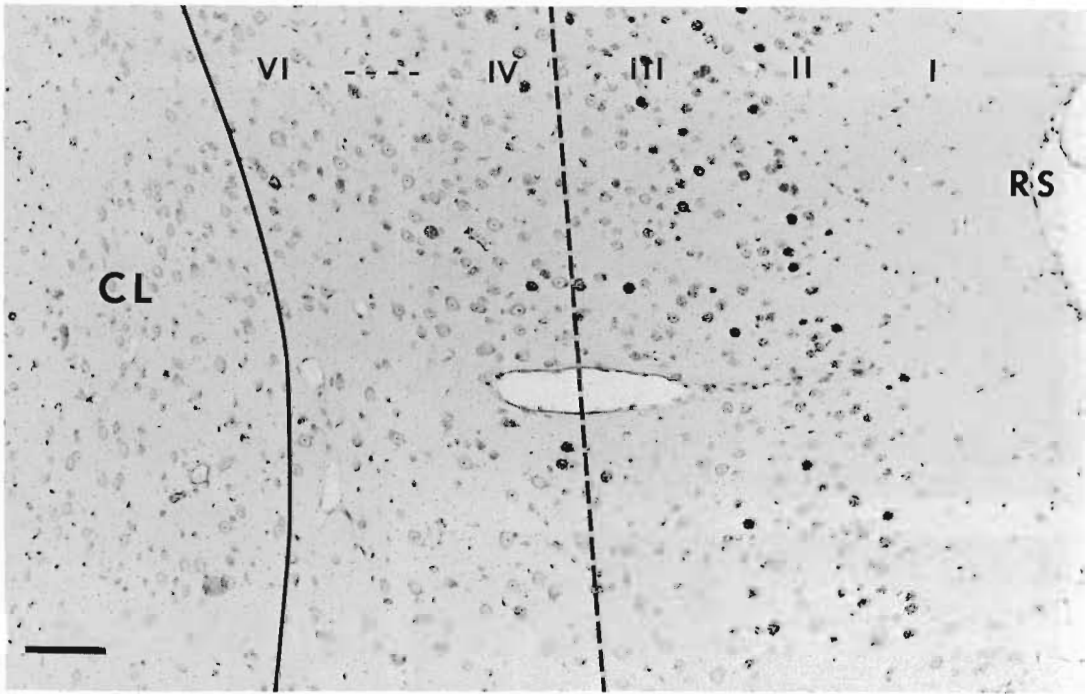


Fig. 11. An autoradiogram of the ventral agranular insular cortex (area 13) at level A5.4 in an animal exposed to $[^3\text{H}]$ thymidine on E16+E17, and killed on P60 (6 μm paraffin section, hematoxylin and eosin, scale = 0.1 mm). The rhinal sulcus (RS) is visible on the left. The claustrum (CL) forms the deep border of this area. Roman numerals refer to layers within the insular cortex; the dashed line indicates how the superficial (I-III) and deep (IV-VI) parts were subdivided for the cell counts. There are proportionately fewer labeled cells located ventrally (toward bottom) and deeply, indicating a combined ventral to dorsal and deep to superficial neurogenetic gradient.

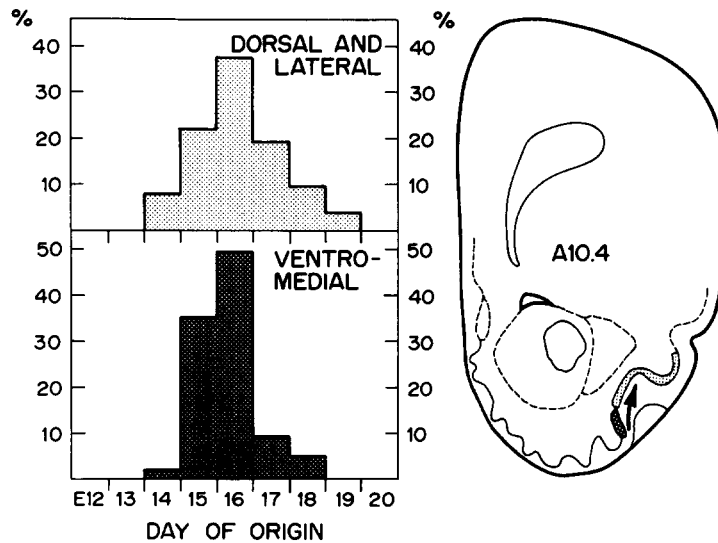


Fig. 7. Neurogenesis of the superficial cells in the piriform cortex at level A10.4. The bar graphs represent the proportion of cells originating over single embryonic days. Ventromedial cells originate earlier than dorsal and lateral cells (arrow in drawing).

An additional trend in labeling patterns was noted but not quantified during the analysis of layer II neurogenesis. Throughout the anterior piriform cortex proper and in the intermediate part of the posterior piriform cortex, layer II is thicker. Superficial cells are less densely packed (IIa) than are deeper cells (IIb). Layer IIa cells tend to become unlabeled sooner (they are slightly older) than the more densely packed cells in IIb (Figs 4B and 6A). This indicates a deviation from the 'inside-out' cortical neurogenetic gradient.

Time of origin of the dorsolateral peduncular cortex

Krieg^{34,35} named the cortex along the ventral lip of the deeply invaginated rhinal sulcus (Fig. 8 and drawings, Fig. 9) area 51b of the piriform cortex. He did not differentiate it from the part of the piriform cortex which is lateral to the amygdala (which he also called area 51b). Today, most anatomists follow Krieg's terminology and consider this area part of the piriform cortex.

As layer II makes a sharp curve to form the lateral prominence in the olfactory peduncle, the high proportion of labeled cells seen in the dorsal part of the piriform cortex suddenly decreases (arrow, Fig. 8A). This sharp drop in the density of layer II labeled cells is considered to be the lateral boundary of a cortical area unique to the adjacent piriform cortex and is termed the dorsolateral peduncular cortex in the following discussion. Most of the superficial cells are unlabeled, while many deep cells are still labeled just beyond the division (Fig. 4B). The density of labeled cells in layer II begins to increase along the medial ventral bank of the rhinal sulcus. A high magnification view of cortex in this area (Fig. 8D) shows that most superficial cells are labeled while deep cells are unlabeled. A tongue-like extension of the lateral superficial cells extends posteriorly to level A9.4 (bottom drawing, Fig. 10). These cells are easily recognized as a densely packed cluster of unlabeled neurons (Fig. 8C) wedged between the piriform cortex below and the ventral insular cortex (Krieg's^{34,35} area 13) above.

Figure 9 shows the neurogenesis of layer II cells in the dorsolateral peduncular cortex throughout the rostrocaudal axis. Cells were counted in unit areas laterally at A9.4 and A10.4, and in lateral, intermediate and medial areas at levels A11.2 and A11.4, respectively. Medial and intermediate areas of cortex along the dorsal part of the olfactory peduncle at level A11.4 are the same as the dorsal transition area immediately posterior to the pars dorsalis of the anterior olfactory nucleus, while the most lateral part of the cortex at A11.4 is the same as the lateral transition area posterior to the pars lateralis. The sign test shows that lateral cells between A11.2 and A9.4 originate simultaneously, and their data are combined in the bottom graph (Fig. 9). The sign test also shows that lateral, intermediate and medial areas of superficial cells originate simultaneously

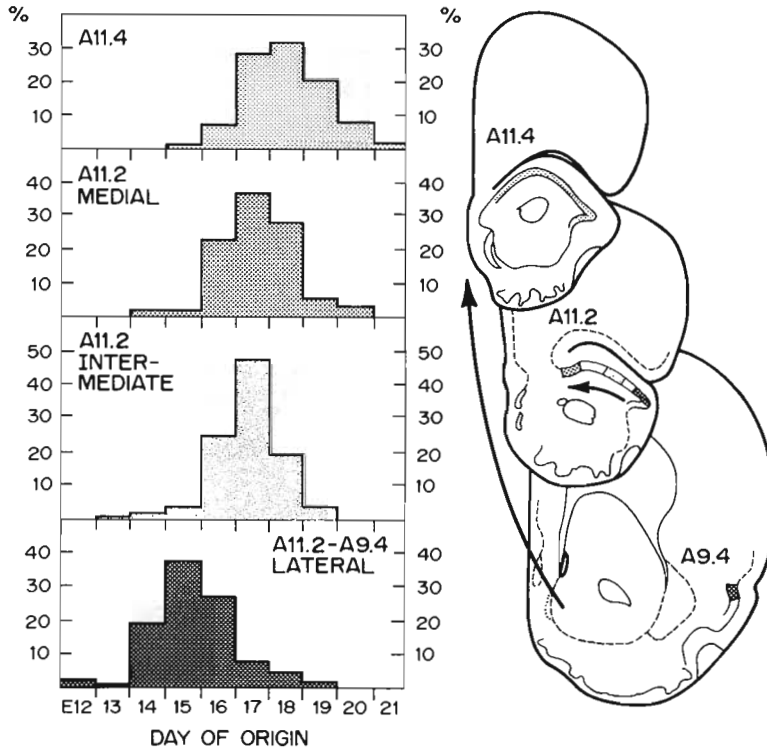


Fig. 9. Neurogenesis of the superficial cells throughout the dorsolateral peduncular cortex. Bar graphs are the proportion of cells generated during single embryonic days. Neurons were counted in the shaded areas shown in the drawings. Lateral cells between levels A11.2 and A9.4 originate simultaneously (data are combined in the bottom graph) and earlier than all other cells; similarly, cells at A11.2 originate earlier than those at A11.4 (arrow to the left of drawings). Within level A11.2 there is an additional lateral to medial neurogenetic gradient (arrow within middle drawing).

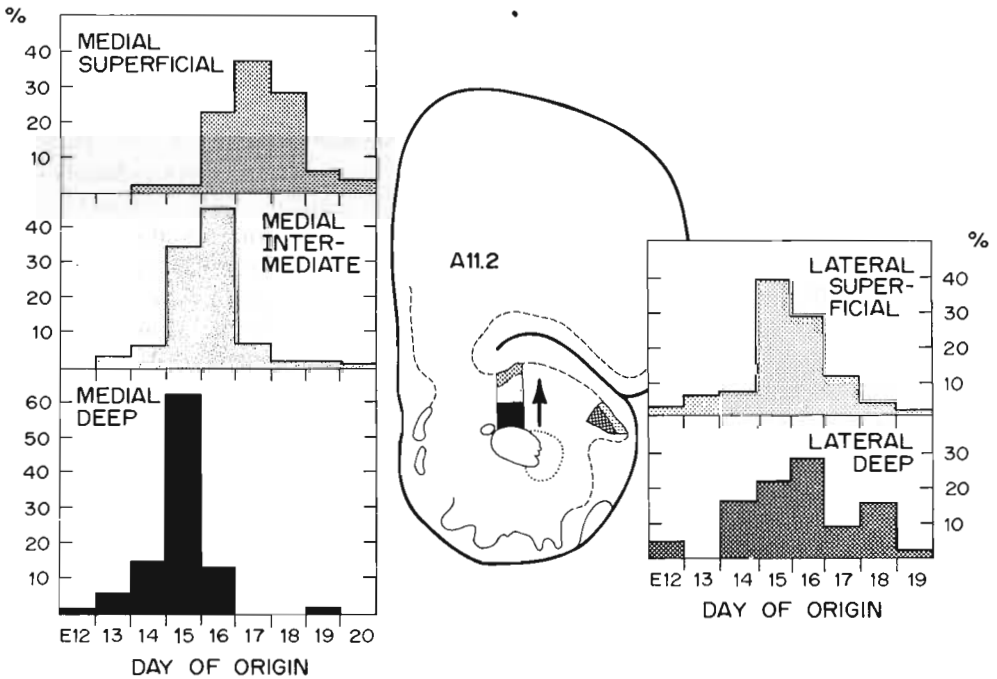


Fig. 10. Neurogenesis along the superficial-deep plane of the dorsolateral peduncular cortex at level A11.2. Bar graphs are the proportion of neurons originating during single embryonic days. There is a strong superficial to deep gradient in the medial area (left panel of graphs, arrow pointing toward surface in drawing). In contrast, the lateral area has no gradient.

at level A11.4, and their data are combined in the top graph (Fig. 9). Neurogenesis occurs in combined lateral to medial and caudal to rostral gradients. The lateral cells in levels A11.2–A9.4 originate significantly earlier ($P < 0.0001$) than intermediate cells at level A11.2, intermediate cells originate earlier than medial cells ($P < 0.001$), and finally, medial cells at A11.2 are significantly older than cells throughout A11.4 ($P < 0.0001$). The gradient is robust, especially when caudolateral cells (83% originate between E12 and E16) are compared with rostral cells (92% originate between E17 and birth).

Superficial–deep gradients in the dorsolateral peduncular cortex are shown in Fig. 10. Deep (layer IV), intermediate (layer III) and superficial (layer II) cells were counted separately in lateral and intermediate strips at level A11.2, while superficial (layer II) and deep (layer III) cells were counted separately in a lateral area at this same level. The sign test shows that a stepwise superficial to deep gradient occurs in both medial (left, Fig. 10) and intermediate strips ($P < 0.0001$). The difference in times of origin between deepest and most superficial cells is dramatic. Most deep cells originate on E15 and before, while most superficial cells originate between E16 and E18. In contrast, the lateral area showed no neurogenetic gradient along the superficial–deep plane (lateral panel of graphs, Fig. 10). The deep cells originate either on E14 (before most superficial cells are generated) or on E18 (after most superficial cells are generated).

Neurogenesis of the ventral agranular insular cortex

The insular cortex is found in the depths of the rhinal sulcus and along its dorsal lip. Krieg^{34,35} divides it into a dorsal part containing granule cells in layer IV (area 14) and a ventral agranular part (area 13). This latter part contains small pyramidal type cells in layer II and medium-sized pyramidal cells in layer III; layer IV is indistinct due to the lack of granule cells and layers V–VI contain larger pyramidal and polymorph cells (Fig. 11). Beneath the deepest layers of the insular cortex are the smaller cells in the claustrum. Between levels A10.4 and A4.4, the ventral agranular insular cortex forms the dorsal boundary of the piriform cortex. Between levels A4.4 and A1.2, it forms the dorsal boundary of the entorhinal cortex. Beyond level A1.2, it blends in with the perirhinal cortex (Krieg's^{34,35} area 35). The posterior two-thirds of the ventral agranular insular cortex receives a direct projection from the olfactory bulb in the opossum,^{41,57} guinea pig,¹² and mouse.^{58,59} This projection has not been officially reported in the rat, but de Olmos *et al.*¹⁸ showed that anterograde transport of horseradish peroxidase from the rat olfactory bulb extended into the depths of the rhinal sulcus, beyond the dorsal limit of the piriform cortex. Due to the high probability of a direct olfactory projection in the rat, neurogenesis in the ventral agranular insular cortex was quantified at 10 levels between A10.4 and A1.2.

Cell counts in all layers of the ventral agranular insular cortex are combined to present an overview of the neurogenetic patterns throughout the rostrocaudal axis (Fig. 12). The sign test shows that between levels A8.4 and A1.2, neurogenesis occurs simultaneously; consequently, these data are combined (bottom graph, Fig. 12). The long expanse of simultaneously arising posterior cells are generated significantly earlier than those at level A9.4 ($P < 0.001$). From A9.4 on, a stepwise caudal to rostral gradient begins so that those at level A9.4 are generated significantly earlier than those at level A10.4 ($P < 0.001$). The gradient is mild: E15–E17 are peak days for neurogenesis throughout the entire insular cortex, with more neurogenesis on E15 posteriorly, and more on E16–E17 anteriorly.

The autoradiogram in Fig. 11 illustrates neurogenetic gradients along the superficial–deep plane. Deep cells in the claustrum and ventral agranular insular cortex are mostly unlabeled, while the superficial layers have a high proportion of labeled cells. At all levels where the insular cortex was quantified, the cells in layers II–III were counted separately from the cells in layers IV–VI (drawing, Fig. 13). The sign test shows a significant ($P < 0.0001$) deep to superficial neurogenetic gradient throughout (Fig. 13 shows data for level A5.4; other levels are not illustrated). The gradient is very strong: 89% of the deep cells originate on or before E15 (75% on E15 alone), while 77% of the superficial cells originate on or after E16.

Between levels A6.4 and A4.4, the ventral insular cortex extends beneath the rhinal sulcus forming a shoulder-like structure overlying the piriform cortex (drawing, Fig. 14). At each of these levels, cells were counted separately in strips through the ventral extension. The sign test shows that ventrally positioned neurons originate significantly ($P < 0.0001$) earlier than those

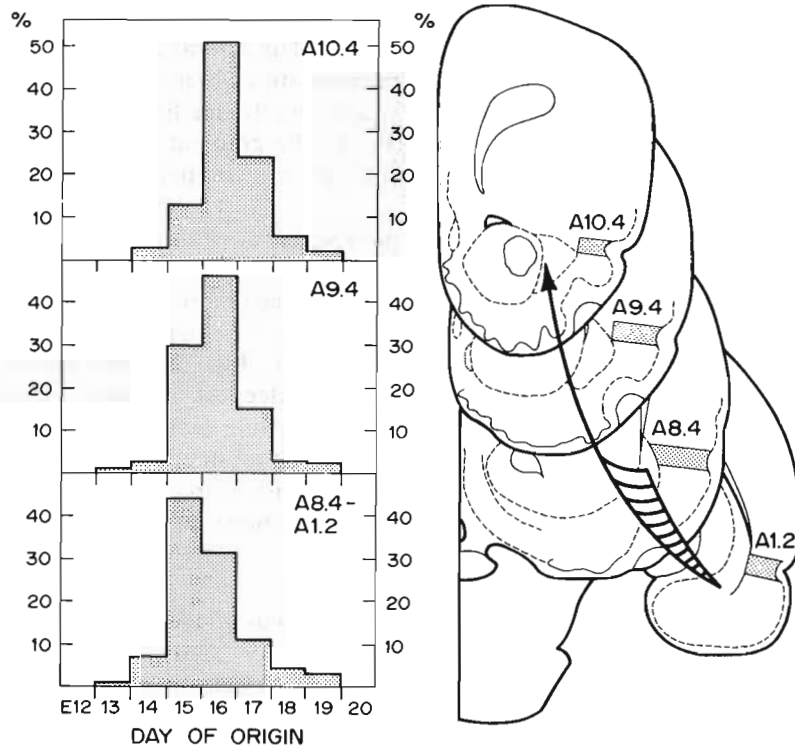


Fig. 12. Neurogenesis throughout the rostrocaudal extent of the ventral agranular insular cortex. Neurons were counted in the shaded areas indicated in the drawings. Bar graphs show the proportion of cells originating during single embryonic days. Cells between levels A8.4 and A1.2 originate simultaneously (data are combined in the bottom graph) and earlier than cells at more anterior levels (arrow between drawings).

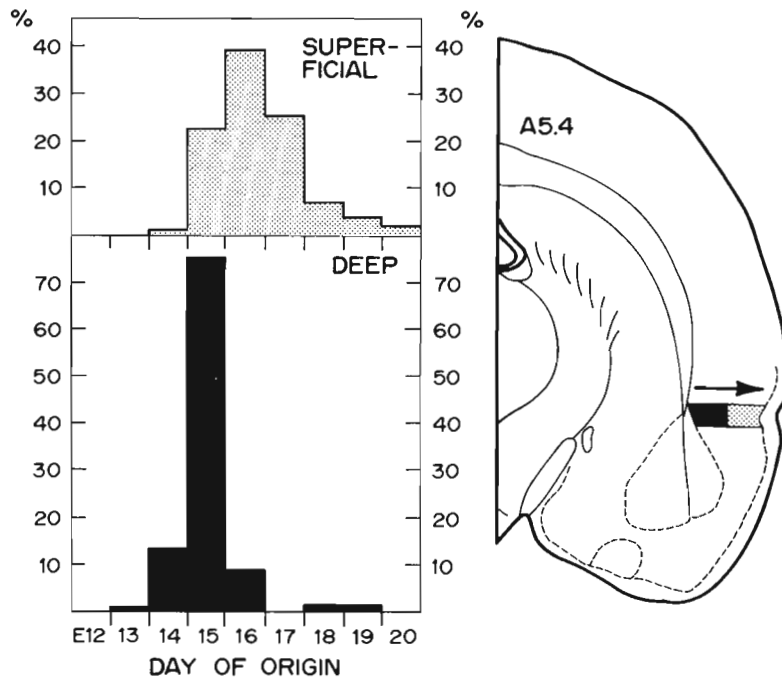


Fig. 13. Neurogenesis along the superficial-deep plane in the ventral agranular insular cortex. Figure 11 shows how the superficial and deep layers were subdivided in the strip. Bar graphs are the proportion of cells originating during single embryonic days. There is a very strong deep to superficial neurogenetic gradient (arrow in drawing).

positioned dorsally at all levels (Fig. 14 shows data for level A6.4; other levels are not illustrated). The gradient is subtle: 61% of the ventral cells are generated on or before E15 (middle graph, Fig. 14), while slightly less (53%) of the dorsal cells are generated during the same time period (top graph, Fig. 14).

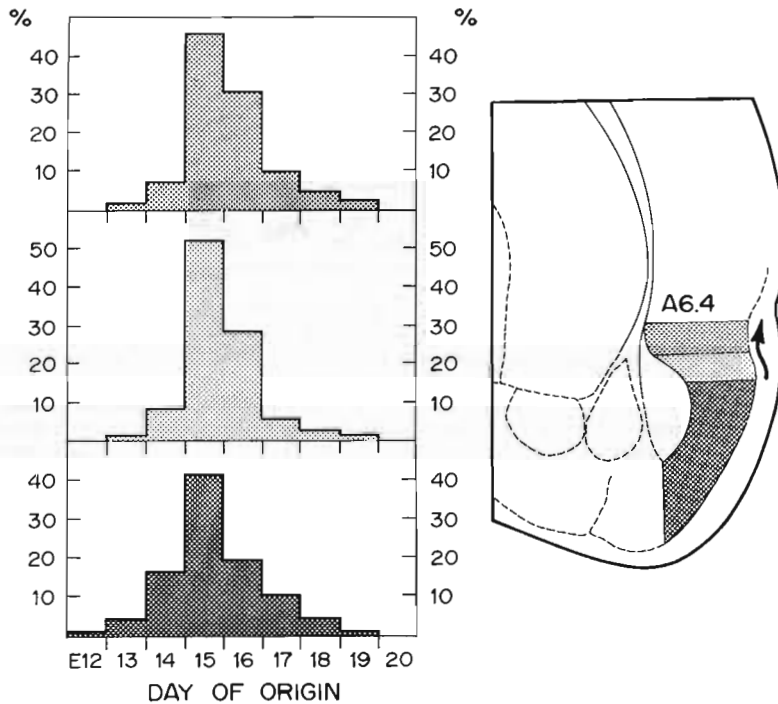


Fig. 14. Neurogenesis in the primary olfactory cortex at level A6.4. Cells were counted (all areas combined) within the shaded areas indicated in the drawing. Bar graphs show the proportion of neurons originating during single embryonic days. Within the insular cortex, there is a ventral to dorsal neurogenetic gradient, but the insular and piriform cortices originate simultaneously.

Comparison of neurogenetic patterns between different subdivisions of the primary olfactory cortex

At levels A6.4 and A11.2 neurogenesis of the piriform cortex as a whole was compared with neurogenesis in the insular cortex and dorsolateral peduncular cortex, respectively. The sign test shows no significant differences between various cortical areas. When compared with the insular cortex, neurogenesis in the piriform cortex is slightly higher on E13–E14 but is simultaneous during the rest of the developmental period (bottom graph, Fig. 14). The same pattern is found at A11.2 when the piriform cortex is compared to the dorsolateral peduncular cortex (data are not illustrated). The sign test also shows that neurogenetic gradients in the ventral insular cortex cannot be significantly related to those in the dorsolateral peduncular cortex. In addition, the ventral lateral entorhinal cortex caudal to the piriform cortex originates nearly simultaneously with the posterior piriform cortex. Thus, all four areas of primary olfactory cortex are generated according to specific intrinsic neurogenetic gradients, apparently independent of each other.

DISCUSSION

Summary of the neurogenetic gradients throughout the primary olfactory cortex

There is a striking similarity in the way the primary olfactory cortical areas are generated along the rostrocaudal axis (Fig. 15). Caudal to level A8.4 (heavy dashed line in Fig. 15), the insular, piriform and lateral entorhinal cortices⁴ originate simultaneously. (The lateral area is the only part of the entorhinal cortex to receive direct input from the olfactory bulb,^{11,12,17,29,41,46,48,57,60,61,64} although two recent studies^{33,58} found a few primary olfactory fibers reach the medial area.) As a

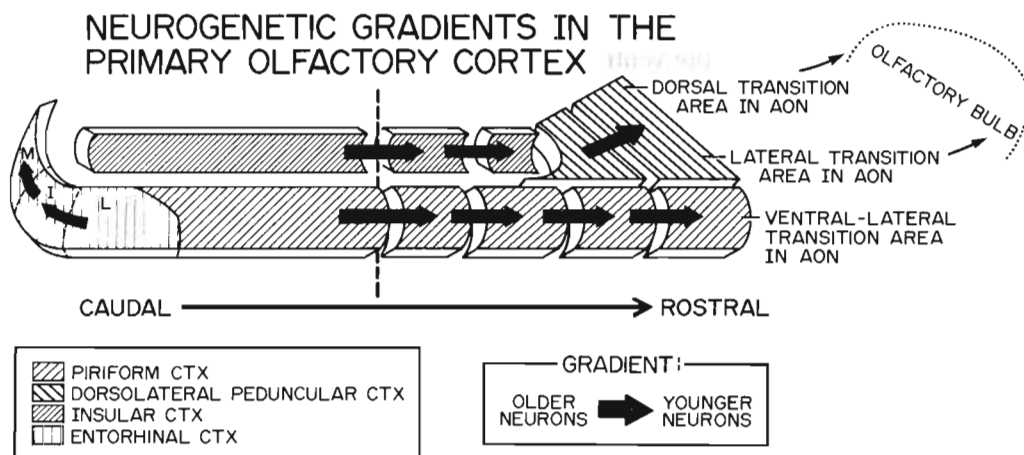


Fig. 15. A diagram summarizing the neurogenetic gradients seen throughout subdivisions (see legend) of the primary olfactory cortex along the rostrocaudal plane. All arrows indicate gradients of neurogenesis. The heavy dashed line represents the approximate location of level A8.4. Caudal to this level, the primary olfactory cortex originates simultaneously and earlier than the cortex located anteriorly. The anterior parts of the primary olfactory cortex, including transition areas and anterior olfactory nucleus, originate in a more prominent stepwise caudal to rostral gradient. Throughout this continuum, younger neurons are positioned nearer to the olfactory bulb; an arrangement which can be related to the primary olfactory projection (Fig. 16). [The lateral (L) entorhinal area originates simultaneously with the posterior piriform cortex but earlier than intermediate (I) or medial (M) areas; this gradient is not related to those in the primary olfactory cortex.]

group, the three caudal parts of primary olfactory cortex originate earlier than rostral parts (indicated by the arrows running across the interface at level A8.4 in Fig. 15). All parts of the rostral primary olfactory cortex show a stepwise and more pronounced caudal to rostral neurogenetic gradient (indicated by arrows running between segments in Fig. 15, also see data in the upper graphs in Figs 1, 5 and 12). We have reported⁹ a pronounced caudal to rostral gradient throughout the olfactory peduncle, probably an extension of what is seen here in the rostral primary olfactory cortex. When the anterior olfactory nucleus and the primary olfactory cortex are taken as a continuum, the youngest neurons are located closest to the olfactory bulb.

Neurogenetic gradients along the rostrocaudal axis in the piriform cortex closely correlate with the observations made by Leonard³⁸ in a developmental study in the hamster. Mature primary olfactory contacts (as judged by long-lasting degeneration agyrophilia) were present as early as postnatal day (P) 2 in the rostral part of the posterior piriform cortex. Olfactory axons grew rapidly throughout the posterior piriform cortex and adult levels of degeneration density were reached by P20. In line with its later neurogenesis, the anterior piriform cortex did not show any mature olfactory contacts until P5, and adult levels were not reached until P33. Also correlating with the caudal to rostral neurogenetic gradient in the piriform cortex, Schwob and Price⁵³ found that associational fibers originating in the posterior piriform cortex developed in advance of those coming from the anterior piriform cortex.

In contrast to their similarity along the rostrocaudal axis, various parts of the primary olfactory cortex have characteristic intrinsic neurogenetic gradients that are independent of each other. The strong lateral to medial gradient in the dorsolateral peduncular cortex (Fig. 10) is not a continuation of the neurogenetic gradients found in layer II of the piriform cortex (Figs 3 and 7). Similarly, the dorsal (younger) to ventral (older) neurogenetic gradient in the ventral agranular insular cortex is not continued in the piriform cortex (Fig. 14). The lateral to medial gradient in the entorhinal cortex (the only arrows in Fig. 15 not pointing to the olfactory bulb) is related to anatomical connections with the hippocampus.⁴ These data imply that each area of primary olfactory cortex is generated by a separate neuroepithelial source. However, similarities in neurogenesis along the rostrocaudal axis (Fig. 15) suggest that developmental events in each neuroepithelium producing a particular part of primary olfactory cortex are linked. We will present evidence below that the rostrocaudal gradient is related to olfactory bulb input.

The intrinsic gradients in layer II of the piriform cortex can be linked to developmental and anatomical observations in the rat. Schwob and Price^{52,53} found that olfactory fibers first reach

the ventromedial part of the piriform cortex, the areas closest to the lateral olfactory tract. The data in Figs 5 and 7 show that superficial cells adjacent to the lateral olfactory tract are older, possibly in connection with their earlier innervation. The area of later originating cells in layer II of the posterior piriform cortex (Fig. 3) may be related to the observation that these neurons die in greater numbers¹² when the olfactory bulb is lesioned.

Using neurogenetic gradients to define the limits of the primary olfactory cortex

All structures receiving direct olfactory input have a plexiform layer (I) on the surface of the brain. Price and his coworkers have studied the laminar arrangement in layer I. Axons leave the lateral olfactory tract and terminate superficially in layer Ia; the associational afferents from other structures in the olfactory system terminate just beneath the primary afferents in layer Ib.^{25,27,39,46,54} This characteristic lamination has made the delineation of primary olfactory cortex a problem in the neuroanatomical literature.³⁰ The piriform cortex is unanimously considered as a cortical structure. There is occasional reference to the cortical organization of the anterior olfactory nucleus²⁸ and portions of the amygdala have been renamed as periamygdaloid cortex.³⁶ In addition, there is a longstanding controversy regarding the cortical nature of the olfactory tubercle.³⁰ At one time or another all parts of the brain receiving a projection from the olfactory bulb have been called 'cortex'. The use of [³H]thymidine autoradiography to examine neurogenetic gradients throughout the olfactory projection field can clearly delineate the limits of the primary olfactory cortex.

The 'inside-out' pattern of neurogenesis which Angevine and Sidman³ first saw in the mouse neocortex is characterized by older cells lying next to the white matter in the deeper cortical layers and progressively younger cells lying in the superficial cortical layers (the often mentioned deep to superficial gradient in this paper). This neurogenetic gradient has since been found in all telencephalic cortical areas thus far examined with [³H]thymidine autoradiography, including various areas in the neocortex^{13,14,20,21,47} and the entorhinal cortex.^{2,4} Thus, this gradient can be regarded as a developmental criterion of telencephalic cortical structures. In addition to the entorhinal cortex, four other structures in the olfactory projection field have the typical 'inside-out' cortical neurogenetic gradient: the present study confirms the observations of Hinds and Angevine³² that (1) the piriform cortex has the 'inside-out' gradient, and extends these observations to (2) the ventral agranular insular cortex and most of (3) the dorsolateral peduncular cortex. The preceding companion paper⁹ reported an 'inside-out' gradient in (4) the dorsal and ventral-lateral transition areas associated with the anterior olfactory nucleus.

On the other hand, four structures getting primary olfactory afferents resemble a cortex but do not have the required neurogenetic gradient: (1) the olfactory tubercle⁸ has no gradient along the superficial-deep plane. Neurogenetic patterns in (2) the cortical nuclei of the amygdala⁵ and (3) anterior olfactory nucleus⁹ show a superficial (older) to deep (younger) gradient, exactly the opposite of the typical cortical gradient. (4) The posterolateral olfactory peduncle is noted for a subgroup of late-originating deep cells (Fig. 10) which throw off the deep to superficial gradient. Perhaps the superficial cells of the dorsolateral peduncular cortex are simply juxtaposed over deep cells that are extensions of the pars lateralis in the anterior olfactory nucleus.⁹

Neurogenetic gradients in target structures correlated with anatomical projections from the olfactory bulb

Since this paper is last in the series to study neurogenetic patterns in the olfactory system, it seems appropriate to summarize data from all of these studies. A hypothetical scheme of the relationship between the neurogenetic gradients in all structures receiving primary olfactory input (target structures) and their connections with the olfactory bulb is shown in Fig. 16. There are caudal to rostral neurogenetic gradients (arrows, Fig. 16) in the primary olfactory cortex and anterior olfactory nucleus. Taken together, these structures constitute the largest target area and are the most well-documented recipients of primary olfactory axons.^{11,12,17,19,25,26,40-42,48,49,55-58,60,61} The amygdala has a rostral (older) to caudal (younger) neurogenetic gradient (arrows, Fig. 16); only the lateral part of the cortical amygdaloid nuclei are contacted by primary olfactory fibers (see Ref. 5 for a review). The olfactory tubercle receives direct olfactory fibers throughout its extent (see Ref. 8 for a review), and has a lateral (older) to medial (younger) gradient (arrows, Fig. 16).

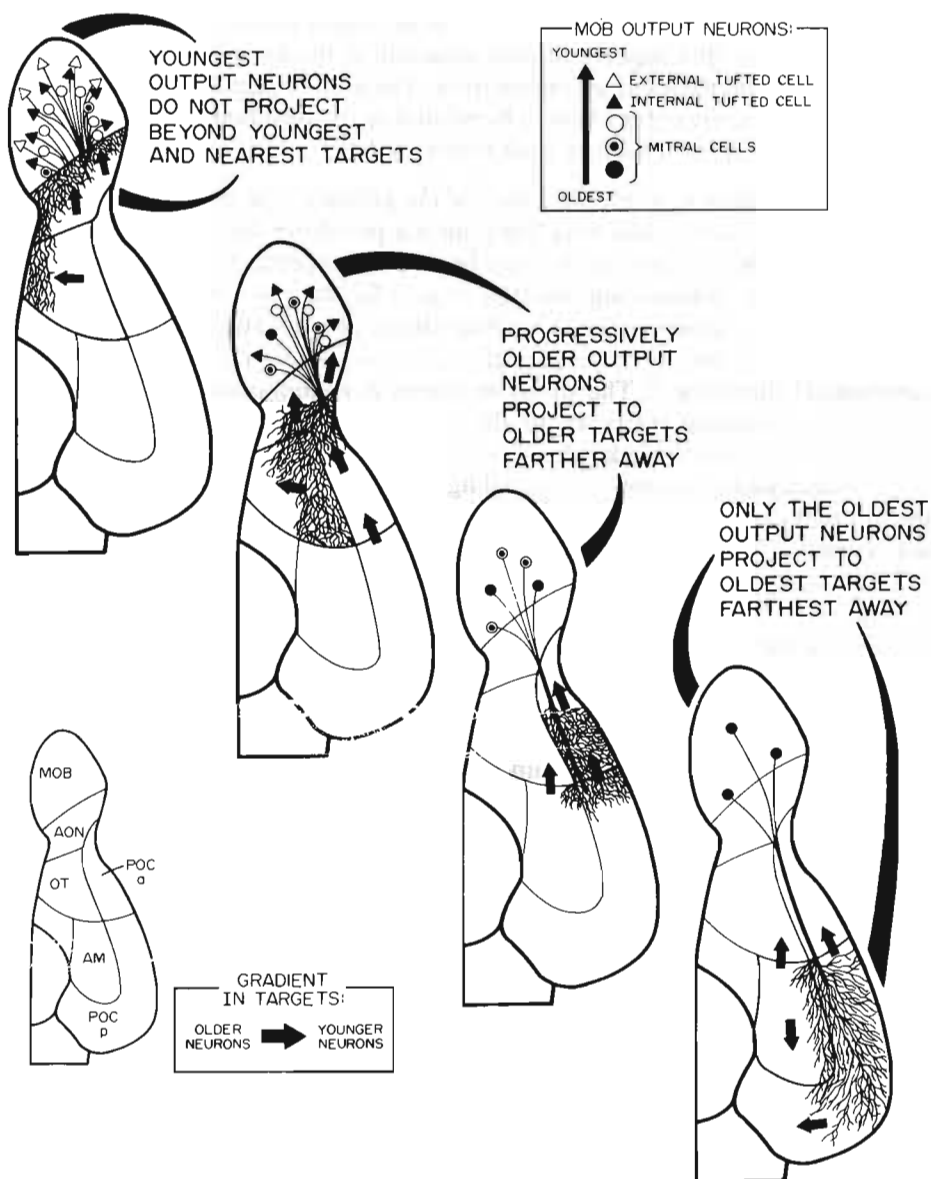


Fig. 16. A diagram indicating the correlation between timetables of neurogenesis in the main olfactory bulb output neurons (upper right legend) and neurogenetic gradients (arrows, lower legend) in target structures reached by primary olfactory axons. (Abbreviations in lower left drawing: AM, amygdala; AON, anterior olfactory nucleus; MOB, main olfactory bulb; OT, olfactory tubercle; POC_a and POC_p, anterior and posterior parts of the primary olfactory cortex.) The projections in drawings along the diagonal show the most caudal extent of axons of youngest output neurons (top drawing), and oldest output neurons (bottom drawing). The oldest mitral cells probably project throughout the entire primary olfactory terminal field; for clarity, the most caudal extent of their axons is shown only in the bottom right drawing. The projections thin out caudally^{26,58} (Bayer *et al.*, unpublished data) presumably due to the decreased number of axons contributed by younger output neurons. Only the oldest mitral cells contact the amygdala and posterior primary olfactory cortex (bottom right drawing).

The output neurons of the main olfactory bulb (mitral and tufted cells) have an intrinsic neurogenetic gradient (upper right legend, Fig. 16). Mitral cells (filled, dotted and empty circles, Fig. 16) are generated mainly between E14 and E17⁶ and lie randomly arranged with respect to age within the mitral cell layer. Tufted cells originate later than the mitral cells.^{6,31} Internal tufted cells (solid triangles, Fig. 16) originate mainly on E16–E17 and are positioned just outside the mitral cell layer; external tufted cells (empty triangles, Fig. 16) originate mainly on E18–E19 and lie closer to the surface of the olfactory bulb.

Neuroanatomical evidence is accumulating which correlates the age of olfactory bulb output neurons with the position of their target zones along the rostrocaudal axis. For example, superficial (youngest) tufted cells project only as far as the pars externa and rostral (youngest) part of the anterior olfactory nucleus.^{50,51} Deeper (older) tufted cells project farther back in the (older) anterior olfactory nucleus and primary olfactory cortex.^{26,49} On the other hand, mitral cells project throughout the olfactory projection field, and their axons constitute the entire projection to the posterior primary olfactory cortex.^{26,49,55} In a horseradish peroxidase (HRP) and [³H]-thymidine double labeling study, Grafe²³ found only the oldest mitral cells project to the posterior piriform cortex in the hamster. We have confirmed these observations in rats: more posterior HRP injection sites retrogradely label only the oldest mitral cells (those originating on or before E15), while more anterior HRP injection sites retrogradely label some younger mitral cells (originating on or after E16) along with older cells (Bayer *et al.*, in preparation). We are continuing these experiments, and plan to inject more rostral parts of the primary olfactory cortex and anterior olfactory nucleus to see if even younger mitral cells become retrogradely labeled. Thus far, these data suggest that progressively younger mitral cells contribute to progressively more anterior projections, and a tentative hypothesis is offered. Within the continuum formed by the anterior olfactory nucleus and the primary olfactory cortex, *the youngest output neurons project to the closest targets which contain the youngest recipient neurons.*

The rostral to caudal neurogenetic gradient in the amygdala has been related to the formation of contacts between olfactory fibers and their target cells (see Ref. 6 for a review). The anterior cortical nucleus of the amygdala contains some of the oldest neurons (generated on E13) to receive direct olfactory input (see Fig. 9 in Bayer⁵). The caudal part of the olfactory projection could first become established when axons of the (presumably) older mitral cells make contacts with the early generated neurons in the anterior cortical nucleus. Both Schwob and Price⁵² and Leonard³⁸ found this part of the olfactory projection field to develop early. The strong lateral to medial neurogenetic gradient in the olfactory tubercle⁸ is in line with the lateral to medial growth of olfactory fibers.^{38,53} Also correlating with the later neurogenesis in the olfactory tubercle, several studies^{26,49,55,56} report that some tufted cells (younger output neurons) contribute to the olfactory tubercle projection.

All of these data, along with other [³H]thymidine autoradiographic studies throughout the central nervous system^{1,4,7} suggest that the time of neuron origin has a direct bearing on the pattern of anatomical connections. Thus, precise patterns of neurogenesis may be an important mechanism used by the developing nervous system (along with others) to reach maturity.

Acknowledgements—I wish to thank Joseph Altman for advice and encouragement. Technical assistance was provided by Peggy Cleary, Vicki Palmore, Lisa Gerard and Gaye Whitham. Figures were prepared by Kathy Shuster and Mark O'Neil. This research was supported by grant NS 19744 from the National Institutes of Health.

REFERENCES

- Altman J. and Bayer S. A. (1981) Time of origin of neurons of the rat inferior colliculus and the relations between cytogenesis and tonotopic order in the auditory pathway. *Exp. Brain Res.* **42**, 411–423.
- Angevine J. B., Jr (1965) Time of neuronal origin in the hippocampal region. *Exp. Neurol.* Suppl. 2, 1–70.
- Angevine J. B., Jr and Sidman R. L. (1961) Autoradiographic study of cell migration during histogenesis of cerebral cortex in the mouse. *Nature* **192**, 766–768.
- Bayer S. A. (1980) The development of the hippocampal region in the rat. I. Neurogenesis examined with [³H]-thymidine autoradiography. *J. comp. Neurol.* **190**, 87–114.
- Bayer S. A. (1980) Quantitative [³H]thymidine radiographic analyses of neurogenesis in the rat amygdala. *J. comp. Neurol.* **194**, 845–875.
- Bayer S. A. (1983) [³H]Thymidine-radiographic studies of neurogenesis in the rat olfactory bulb. *Exp. Brain Res.* **50**, 329–340.
- Bayer S. A. (1984) Neurogenesis in the rat neostriatum. *Int. J. devl Neurosci.* **2**, 163–175.
- Bayer S. A. (1985) Neurogenesis in the olfactory tubercle and islands of Calleja in the rat. *Int. J. devl Neurosci.* **3**, 135–147.
- Bayer S. A. (1986) Neurogenesis in the anterior olfactory nucleus and its associated transition areas in the rat brain. *Int. J. devl Neurosci.* **4**, 225–249.
- Bayer S. A. and Altman J. (1974) Hippocampal development in the rat: cytogenesis and morphogenesis examined with autoradiography and low-level X-irradiation. *J. comp. Neurol.* **158**, 55–80.
- Broadwell R. D. (1975) Olfactory relationships of the telencephalon and diencephalon in the rabbit. I. An autoradiographic study of the efferent connections of the main and accessory olfactory bulbs. *J. comp. Neurol.* **163**, 329–346.

12. Carlsen J., de Olmos J. and Heimer L. (1982) Tracing two-neuron pathways in the olfactory system by the aid of transneuronal degeneration: projections to the amygdaloid body and hippocampal formation. *J. comp. Neurol.* **208**, 196–208.
13. Caviness V. S., Jr (1982) Neocortical histogenesis in normal and reeler mice: a developmental study based upon [³H]thymidine autoradiography. *Devl Brain Res.* **4**, 293–302.
14. Caviness V. S., Jr and Sidman R. L. (1973) Time of origin of corresponding cell classes in the cerebral cortex of normal and reeler mutant mice: an autoradiographic analysis. *J. comp. Neurol.* **148**, 141–151.
15. Conover W. J. (1971) *Practical Nonparametric Statistics*. John Wiley, New York.
16. Cragg B. G. (1961) Olfactory and other afferent connections of the hippocampus in the rabbit, rat and cat. *Exp. Neurol.* **3**, 588–600.
17. Davis B. J., Macrides F., Youngs W. M., Schneider S. P. and Rosene D. L. (1978) Efferents and centrifugal afferents of the main and accessory olfactory bulbs in the hamster. *Brain Res. Bull.* **3**, 59–72.
18. de Olmos J., Hardy H. and Heimer L. (1978) The afferent connections of the main and the accessory olfactory bulb formations in the rat: an experimental HRP-study. *J. comp. Neurol.* **181**, 213–244.
19. Devor M. (1976) Fiber trajectories of olfactory bulb efferents in the hamster. *J. comp. Neurol.* **166**, 31–48.
20. Fernandez V. (1969) An autoradiographic study of the development of the anterior thalamic group and limbic cortex in the rabbit. *J. comp. Neurol.* **136**, 423–452.
21. Fernandez V. and Bravo H. (1974) Autoradiographic study of development of the cerebral cortex in the rat. *Brain Behav. Evol.* **9**, 317–322.
22. Girgis M. and Goldby F. (1967) Secondary olfactory connexions and the anterior commissure in the coypu (*Myocastor coypus*). *J. Anat.* **101**, 33–44.
23. Grafe M. R. (1983) Developmental factors affecting regeneration in the central nervous system: early but not late formed mitral cells reinervate olfactory cortex after neonatal tract section. *J. Neurosci.* **3**, 617–630.
24. Gray P. A. (1924) The cortical lamination pattern of the opossum. *Didelphys virginiana*. *J. comp. Neurol.* **37**, 221–263.
25. Haberly L. and Behan M. (1983) Structure of the piriform cortex of the opossum. III. Ultrastructural characterization of synaptic terminals of association and olfactory bulb afferent fibers. *J. comp. Neurol.* **219**, 448–460.
26. Haberly L. B. and Price J. L. (1977) The axonal projection patterns of the mitral and tufted cells of the olfactory bulb in the rat. *Brain Res.* **129**, 152–157.
27. Haberly L. B. and Price J. L. (1978) Association and commissural fiber systems of the olfactory cortex of the rat. I. Systems originating in the piriform cortex and adjacent areas. *J. comp. Neurol.* **178**, 711–740.
28. Haberly L. B. and Price J. L. (1978) Association and commissural fiber systems of the olfactory cortex of the rat. II. Systems originating in the olfactory peduncle. *J. comp. Neurol.* **181**, 781–808.
29. Heimer L. (1968) Synaptic distribution of centripetal and centrifugal nerve fibers in the olfactory system of the rat. An experimental anatomical study. *J. Anat.* **103**, 413–432.
30. Heimer J. (1978) The olfactory cortex and the ventral striatum. In *Limbic Mechanisms: The Continuing Evolution of the Limbic System Concept* (eds Livingston K. E. and Hornykiewicz O.), pp. 95–187. Plenum Press, New York.
31. Hinds J. W. (1967) Autoradiographic study of histogenesis in the mouse olfactory bulb. I. Time of origin of neurons and neuroglia. *J. comp. Neurol.* **134**, 287–304.
32. Hinds J. W. and Angevine J. B., Jr (1965) Autoradiographic study of histogenesis in the area pyriformis and claustrum of the mouse. *Anat. Rec.* **151**, 456–457 (Abstract).
33. Kosel K. C., Van Hoesen G. W. and West J. R. (1981) Olfactory bulb projections to the parahippocampal cortices in the rat. *J. comp. Neurol.* **198**, 467–482.
34. Krieg W. J. S. (1946) Connections of the cerebral cortex. I. The albino rat. A. Topography of the cortical areas. *J. comp. Neurol.* **84**, 221–275.
35. Krieg W. J. S. (1946) Connections of the cerebral cortex. I. The albino rat. B. Structure of the cortical areas. *J. comp. Neurol.* **84**, 277–323.
36. Krettek J. E. and Price J. L. (1978) A description of the amygdaloid complex in the rat and cat with observations on intra-amygdaloid axonal connections. *J. comp. Neurol.* **178**, 255–280.
37. LeGros Clark W. E. and Mayer M. (1947) Terminal connexions of the olfactory tract in the rabbit. *Brain* **70**, 304–328.
38. Leonard C. M. (1975) Developmental changes in olfactory bulb projection revealed by degeneration agyrophilia. *J. comp. Neurol.* **162**, 467–486.
39. Luskin M. B. and Price J. L. (1983) The topographic organization of associational fibers of the olfactory system in the rat, including centrifugal fibers to the olfactory bulb. *J. comp. Neurol.* **216**, 264–291.
40. Macrides F., Davis B. J., Youngs W. M., Nadi N. S. and Margolis F. L. (1981) Cholinergic and catecholaminergic afferents to the olfactory bulb in the hamster: a neuroanatomical, biochemical and histochemical investigation. *J. comp. Neurol.* **203**, 497–516.
41. Meyer R. (1981) Central connections of the olfactory bulb in the American opossum (*Didelphys virginiana*): a light microscopic degeneration study. *Anat. Rec.* **201**, 141–156.
42. Ojima H., Mori K. and Kishi K. (1984) The trajectory of mitral cell axons in the rabbit olfactory cortex revealed by intracellular HRP injection. *J. comp. Neurol.* **230**, 77–87.
43. O'Leary J. L. (1937) Structure of the primary olfactory cortex of the mouse. *J. comp. Neurol.* **67**, 1–31.
44. Pellegrino L. J., Pellegrino A. S. and Cushman A. J. (1979) *A Stereotaxic Atlas of the Rat Brain*, 2nd edn. Plenum Press, New York.
45. Powell T. P. S., Cowan W. M. and Raisman G. (1965) The central olfactory connexions. *J. Anat.* **99**, 791–813.
46. Price J. L. (1973) An autoradiographic study of complementary laminar patterns of termination of afferent fibers to the olfactory cortex. *J. comp. Neurol.* **150**, 87–108.
47. Rakic P. (1974) Neurons in Rhesus monkey visual cortex: systematic relation between time of origin and eventual disposition. *Science* **183**, 425–427.
48. Scalia F. and Winans S. S. (1975) The differential projections of the olfactory bulb and accessory olfactory bulb in mammals. *J. comp. Neurol.* **161**, 31–56.
49. Schneider S. P. and Scott J. W. (1983) Orthodromic response properties of rat olfactory bulb mitral and tufted cells correlate with their projection patterns. *J. Neurophysiol.* **50**, 358–378.

50. Schoenfeld T. A. and Macrides F. (1984) Topographic organization of connections between the main olfactory bulb and pars externa of the anterior olfactory nucleus in the hamster. *J. comp. Neurol.* **227**, 121–135.
51. Schoenfeld T. A., Marchand J. E. and Macrides F. (1985) Topographic organization of tufted cell axonal projections in the hamster main olfactory bulb: an intrabulbar associated system. *J. comp. Neurol.* **235**, 503–518.
52. Schwob J. E. and Price J. L. (1978) The cortical projection of the olfactory bulb: development in fetal and neonatal rats correlated with quantitative variations in adult rats. *Brain Res.* **151**, 369–374.
53. Schwob J. E. and Price J. L. (1984) The development of axonal connections in the central olfactory system of rats. *J. comp. Neurol.* **223**, 177–202.
54. Schwob J. E. and Price J. L. (1984) The development of lamination of afferent fibers to the olfactory cortex in rats with additional observations in the adult. *J. comp. Neurol.* **223**, 203–222.
55. Scott J. W. (1981) Electrophysiological identification of mitral and tufted cells and distribution of their axons in the olfactory system of the rat. *J. Neurophysiol.* **46**, 918–931.
56. Scott J. W., McBride R. L. and Schneider S. P. (1980) The organization of projections from the olfactory bulb to the piriform cortex and olfactory tubercle in the rat. *J. comp. Neurol.* **194**, 519–534.
57. Shammah-Lagnado S. J. and Negrao N. (1981) Efferent connections of the olfactory bulb in the opossum (*Didelphys marsupialis aurita*): a Fink-Heimer study. *J. comp. Neurol.* **201**, 51–63.
58. Shipley M. T. and Adamek G. D. (1984) The connections of the mouse olfactory bulb: a study using orthograde and retrograde transport of wheat germ agglutinin conjugated to horseradish peroxidase. *Brain Res. Bull.* **12**, 669–688.
59. Shipley M. T. and Geinisman Y. (1984) Anatomical evidence for convergence of olfactory, gustatory, and visceral afferent pathways in mouse cerebral cortex. *Brain Res. Bull.* **12**, 221–226.
60. Skeen L. C. and Hall W. C. (1977) Efferent projections of the main and the accessory olfactory bulb in the tree shrew (*Tupaia glis*). *J. comp. Neurol.* **172**, 1–36.
61. Turner B. H., Gupta K. C. and Mishkin M. (1978) The locus and cytoarchitecture of the projection areas of the olfactory bulb in *Macaca mulatta*. *J. comp. Neurol.* **177**, 381–396.
62. Valverde F. (1963) Studies in the forebrain of the mouse. Golgi observations. *J. Anat.* **97**, 157–180.
63. Valverde F. (1965) *Studies on the Piriform Lobe*. Harvard University Press, Cambridge, MA.
64. White L. E., Jr (1965) Olfactory bulb projections of the rat. *Anat. Res.* **152**, 465–480.